Meteorol Atmos Phys 102, 159–171 (2008)
DOI 10.1007/s00703-008-0320-9
Printed in The Netherlands

Meteorology and Atmospheric Physics

[1] CNRM-GAME, CNRS Meteo-France, Toulouse, France
[2] Department of Geography, University of Western Ontario, London, Ontario, Canada

Simulation of fall and winter surface energy balance over a dense urban area using the TEB scheme

G. Pigeon[1,*], M. A. Moscicki[2,*], J. A. Voogt[2], V. Masson[1]

With 4 Figures

Received 5 August 2007; Accepted 28 April 2008
Published online 20 August 2008

Summary

The Town Energy Balance (TEB) scheme computes the surface energy balance for urban areas. It is intended to be coupled with atmospheric models for numerical weather prediction, air quality forecasts or research applications. Up to now, it has been evaluated for dry and hot seasons over light industrial (Vancouver) or dense urban (Mexico City, Marseille) areas. In this study, the evaluation of TEB is extended to two other seasons, fall and winter, using measurements conducted over a dense urban area of Toulouse (France) instrumented from February 2004 to March 2005. Most of the model outputs were measured (individual components of the net radiation, sensible heat flux) as well as state variables of the model (surface temperatures of roofs, roads, walls). Great care has been taken in the design of the surface temperature measurement strategy in order to provide comparable observations to modelled estimates. Focusing on the fall and winter season, this study also proposes an evaluation of the parameterization of anthropogenic heat sources against an inventory of energy consumption.

1. Introduction

Modelling of the urban climate has become of great interest for several reasons. Urban climates impact the majority of the world's population, so they are strategic topics of research. For example, during the 2003 heat wave in Europe, the urban heat island (UHI) strengthened the heat stress conditions in large cities like Paris. The atmospheric dispersion of pollutants in urban areas is affected by the specific turbulence characteristics in the urban boundary layer (Batchvarova and Gryning 2006). Finally, the prospect of large scale climate change calls for an adaptation of urban areas to the future environment (Best 2006; Hallegatte et al. 2007). A large number of models, using different approaches, have been developed recently to reproduce the processes that govern urban climate (for a review see Masson 2006). But beyond this first step of development, only a few models have been extensively evaluated against field measurements of fluxes and surface temperatures (Grimmond and Oke 1999a; Masson et al. 2002; Lemonsu et al. 2004; Hamdi and Schayes 2005).

The Town Energy Balance (TEB) model (Masson 2000) is a single-layer urban canopy model (Masson 2006). It represents the urban surface by a simplified set of urban canyons of all possible directions and is forced by atmospheric data provided either by observations (off-line mode) or by an atmospheric model (coupled

[*] These authors equally contribute to this work.

Correspondence: Grégoire Pigeon, Meteo-France, CNRM/GMEI/4M, 42, av. G. Coriolis, 31057 Toulouse Cedex, France (E-mail: gregoire.pigeon@meteo.fr)

mode). TEB considers the influence of the street canyon geometry on both short-wave and long-wave radiation. It establishes a separate energy budget for each surface (road, wall, roof). The heat transfers through the wall and the roof are represented as well as the exchanges of heat with the inside of the building. The final outputs of TEB are the exchanges of heat, momentum and mass at the top of the canopy weighted as a function of the surface fraction occupied by the canyons and the roofs. It has been designed to be easily transferable from research applications to numerical weather prediction systems or climate models. TEB has been evaluated against field data sets in a light industrial area (Masson et al. 2002) of Vancouver and dense urban areas of Mexico City (Masson et al. 2002), Marseille (Lemonsu et al. 2004; Roberts et al. 2006) and Łódź (Offerle et al. 2005). These evaluations show that TEB is able to reproduce well the exchanges of heat and momentum between the urban surface and the atmosphere. One limitation of TEB evaluation is that the measurement period is restricted to summer conditions for the studies of Masson et al. (2002), Lemonsu et al. (2004) and Roberts et al. (2006). In this study, our objective is to conduct an evaluation of TEB for fall and winter over a dense urban area of Toulouse, where micrometeorological measurements were conducted during the CAPITOUL field program (Masson et al. 2008). For the first time in this study, the parameterization of the anthropogenic heat releases is evaluated against an inventory of energy consumption. The paper first presents the methods adopted for this evaluation including the characteristics of the studied area, and the observation and simulation strategies. Then, the evaluation of the different fluxes (net radiation, sensible and anthropogenic heat flux) and the surface temperature of each facet are presented.

2. Methods

2.1 TEB evaluation strategy

Our objective was to conduct the TEB evaluation with the same methods as in Masson et al. 2002 and in Lemonsu et al. 2004, but for a longer time period. In this mode, TEB computes energy fluxes for the urban fraction and ISBA (Interaction Soil–Biosphere–Atmosphere model/Noilhan and Planton 1989) for the other types of surface cover. The simulations were performed in an offline mode; that is the model is not coupled with an atmospheric mesoscale model but instead the atmospheric forcing is given by observations above the canopy layer. This mode of running TEB reduces errors due to the atmospheric forcing and makes it possible to run long term simulations. The forcing parameters necessary to run TEB are: air temperature, specific humidity, atmospheric pressure, incoming global radiation, incoming long-wave radiation, precipitation rate and wind speed. TEB outputs the energy fluxes above the canopy layer at the blending height (from two to four times the average building heights in accordance with the horizontal separation between buildings) and the state variables are the temperatures of the wall, the roof and the road. The evaluation of TEB uses the measurement of the sensible heat flux, the net radiation, the anthropogenic heat flux and the surface temperatures of canyon walls, roads and roofs. This evaluation strategy was incorporated in the design of the CAPITOUL field program: all the variables necessary to run and evaluate TEB were measured in a dense urban area of the old centre of Toulouse (Masson et al. 2008; Pigeon et al. 2007).

2.2 Study area

The study area is located in the old centre of Toulouse where measurements (see following section) were conducted during the CAPITOUL field program (Masson et al. 2008). In this neighbourhood, vegetation is very scarce (8%, Table 1) and buildings are typically 4–5 stories. The area

Table 1. Characteristics of the area (average over the 500-m radius circle around the surface energy balance station)

Parameter	Value
Building pad[1]	0.54
Road pad	0.38
Tree pad	0.06
Grass pad	0.02
Building height (m)	14.9
Aspect ratio[2]	1.4

[1] Plan area density
[2] Ratio between the height of the buildings and the width of the streets

Table 2. Characteristics of the wall, the roof and the road used in the simulations

	Surface albedo α	Surface emissivity ε	Layer	Depth (m)	Material	Heat capacity (10^6 J m^{-3} K^{-1})	Thermal conductivity (W m^{-1} K^{-1})
Wall	0.25	0.92	1	0.01	Red bricks	1.58	1.15
			2	0.05			
			3	0.18			
			4	0.05			
			5	0.01			
Roof	0.15	0.90	1	0.01	Red tiles	1.58	1.15
			2	0.05			
			3	0.02	Wood	2.20	0.20
			4	0.01			
Road	0.08	0.95	1	0.01	Asphalt	1.74	0.82
			2	0.04			
			3	0.20	Stone aggregate	2.00	2.1
			4	1.00	Gravel and soil	1.40	0.4

is classified as Urban Climate Zone 2 (UCZ2) according to Oke (2006). The quantification of the urban parameters of this area is presented in Table 1. Values are averages over the 500-m radius circle around the surface energy balance station. Parameters were estimated from the Geographical Information System of Toulouse which is composed of a three dimensional vector database of the buildings and aerial ortho-rectified photography at a 0.25 m resolution. Buildings in the centre of Toulouse are very homogeneous and most of them are from the 19th century. For that reason, walls are built with bricks and most are not insulated as well as the roofs. Most roofs are covered with tiles (constructed from the same clay material as the bricks). The thermal and radiative characteristics of the walls, roads and roofs are presented in Table 2.

2.3 Observations

a) Forcing parameters

The forcing parameters (for details on the instrumentation see Pigeon et al. 2007; Masson et al. 2008) were measured at the top of a pneumatic tower installed on a building roof, 20 m above street level. Because of the mechanical characteristics of the tower, its height had to be adjusted depending on the wind (or thunderstorm) conditions between three positions: 28 m (above the terrace) for fair weather, 18 m for wind speeds between 16.7 and 25 m s^{-1} and 6 m for stronger wind speeds. The tower was operated for a one year period from 20 February 2004 to 28 February 2005. For periods when forcing data from the tower were missing, gaps were filled with observations from a meteorological station situated 5 km from the site in a suburban area. The temperature and the relative humidity recorded at this station were corrected for the typical difference in the daily cycle between the two sites. This gap filling of missing forcing observations from the tower is important to ensure a continuity of the simulation and avoid initialisation problems. Furthermore, the evaluation of the model was omitted for the periods when the forcing observations were missing since the observed fluxes were not available. Since the tower was not always operated at the same height (and the station to fill the missing data was not at the same height), wind speed, which determines the turbulent exchange coefficients, has been normalized to the highest extension of the tower using the log law profile for neutral conditions, a displacement height (z_d) of $0.7z_H$ (building height) and a roughness length (z_0) of $0.1z_H$ (Grimmond and Oke 1999b). The assumption of neutral stability to adjust the wind speed is justified because it best characterizes the stability during times of moderate to strong winds when the tower height is reduced.

b) Energy fluxes

The fluxes of net radiation (Q^*) and sensible heat (Q_H) were measured above the canopy at the top of the tower, in the inertial layer, for comparison with the outputs of the TEB model. Net radiation was measured with a four component radiometer (CNR1; see Pigeon et al. 2007 for a list of instruments). Sensible heat fluxes were estimated using

Table 3. Characteristics of the streets instrumented during the CAPITOUL field campaign

Road	Azimuth (°/North)	Mean aspect ratio	Road sky view factor	Wall view[1]	% brick	% concrete	% glass	Weighted emissivity	Wall sky view factor
Alsace	0	1.4	0.309	270	80	0	20	0.932	0.237
				90	0	50	50	0.895	
Pomme	120	1.8	0.231	210	50	0	50	0.935	0.188
				30	80	0	20	0.932	
Rémusat	60	1.8	0.276	150	20	50	30	0.893	0.229
				330	60	0	40	0.934	0.205

[1] Direction to which the wall is pointing (°/North)

eddy-covariance techniques for half hourly periods. Wind components were first corrected with two successive rotations (azimuth and pitch corrections). Then before computing the covariance, the time series were high-pass filtered with a recursive filter according to McMillen (1988), with the filter parameter set to 200 s.

c) Surface temperatures

Surface temperatures are state variables of the TEB model. For that reason, their evaluation is of great interest and they are among the parameters that could be estimated with satellites and assimilated by TEB. TEB represents the urban surface by the repetition of the urban canyon structure (Masson 2000). TEB computes separate energy budgets for the road, the roof and the wall. For each of these structures, a mean surface temperature is computed. In TEB computations, all the directions for the urban canyon are considered and surface temperatures are averaged over all these directions. As surface temperatures strongly depend on the orientation of the streets and its geometry, it is important that measurements constitute a representative sample of all the possible directions and geometries. In CAPITOUL, three streets, between which the azimuth varies by 60°, have been instrumented (Table 3) with infra-red thermometers (IRT). In each street, three IRTs were installed to measure the surface temperature of the two walls and the road. The roof surface temperature was measured for a single tile roof. The IRT was set up two meters above the top of the roof so that both sides of the roof are in its field of view (FOV).

In order to make meaningful comparisons between measurements and the model, the raw data must undergo several processing steps. First, measurements were corrected using individual sensor calibrations from a black-body calibration facility. Secondly, because the output produced by TEB is a kinetic temperature but the thermometers report an apparent surface temperature, a data correction for emissivity was needed. Emissivity values for the walls of the canyons were estimated by using a weighted average based on the types of building material making up the entire surface of the wall under study. The emissivity values of the various wall materials (brick = 0.93, concrete = 0.85, glass = 0.94) were obtained from ASHRAE (1989). The characteristics and the overall emissivity of each wall are shown in Table 3. The emissivity of the asphalt roads (0.95) and the tile roofs (0.90) was obtained from values in the literature (Oke 1987; Masson et al. 2002; Lemonsu et al. 2004). As in Voogt and Oke (1998) and Kobayashi and Takamura (1994), the radiation received from a canyon wall (road, respectively) was approximated using one reflection event from the opposite wall and the road (from both walls, respectively). Emissivity corrections for the roofs only require accounting for reflection of longwave radiation from the sky. For each surface, view factors of the sky and the other surfaces reflecting longwave radiation were calculated as in Noilhan (1981) and are reported in Table 3.

Next, for road and wall surface temperatures, a weighting procedure was applied to take into account (i) the variable geometry (canyon aspect ratio) of the study canyons and (ii) the canyon orientations. This weighting procedure is intended to provide an appropriately averaged wall and road temperature for comparison with the TEB output, which assumes any canyon orientation is possible with equal probability (Masson 2000) for a single specified canyon aspect ratio. The weighting scheme is based on receipt of short-

wave radiation on the canyon walls and floor calculated using a detailed urban canyon model (Krayenhoff and Voogt 2007). The weighting scheme provides improvements to the model evaluation statistics of up to 0.3 °C compared to the use of an arithmetic weighting scheme (Moscicki 2007).

For the road surface temperatures, a final processing step has been applied. At times, vehicles passed through the field of view of the IRTs thus compromising their ability to accurately measure the road surface temperatures since the IRTs would instead view the top or the side of the vehicles. A methodology has been developed to correct for the effect of traffic on the measurements of the IRTs and is presented in Appendix A. Depending on the traffic intensity, the corrections are up to a few tenths of a degree.

2.4 Estimation of anthropogenic heat in TEB and comparison with an inventory of energy consumption

TEB takes into account three sources of anthropogenic heat (Q_F): releases from traffic, releases from industry, and releases from space heating. The two first sources of Q_F need to be prescribed in TEB as additional sensible or latent flux sources. The central area of Toulouse presented in this study is free of industrial activities. Traffic releases over the 500-m radius circle area around the instrumented tower have been estimated using traffic counts from two automatic counters located on two major roads of the area (one counter is on Alsace road close to the measurement site). Traffic intensity was multiplied by the length of the different sections of road within the 500 m study area and the fuel economy of the vehicles (for more details on the methodology see Pigeon et al. 2007). With these data, a mean annual traffic heat release of 8 W m^{-2} was computed for the area. Currently, in TEB, this value is roughly modulated by the diurnal cycle: all the releases are considered to occur during the daylight hours only and no heat release associated with traffic occurs by night. Consequently the day heat flux associated to traffic is equal to the mean value multiplied by the inverse of daylight hours ratio.

The other releases from buildings were estimated with an inventory of energy consumption measured at a 100 m resolution over the entire agglomeration of Toulouse for the period of the CAPITOUL field campaign (Pigeon et al. 2007). These deliveries of energy are supposed to instantaneously compensate heat loss from the buildings as in Ichinose et al. (1999) and Sailor and Lu (2006). This inventory was built on the real consumption of electricity and gas which represent 90% of the energy use in Toulouse buildings. For the other sources of energy (domestic fuel, wood and others), mean annual values from 2001 were available. To estimate the consumption during CAPITOUL, these values were weighted by the ratio of 2001 mean annual consumption of gas to the mean consumption of gas during CAPITOUL. The spatial distribution of the consumption of energy has been computed first, as a function of the mean annual energy consumption known for the different districts of the urban area and second, as a function of the plan area density of buildings (see Pigeon et al. 2007 for more details). Over the area presented in this study, releases from buildings have been shown to be the dominant component of Q_F during fall and winter (Pigeon et al. 2007). They result from space heating and all other domestic uses. In TEB, to mimic space heating, a fixed minimum internal building temperature of 19 °C is specified (Masson 2000; Masson et al. 2002). During fall or winter, internal wall and roof surface temperatures often have values below this threshold, and the heat flux between the internal volume of the building and the wall (or the roof) is directed out of the building. This parameterization has never been evaluated before this study. Hence, a new diagnostic has been computed in the model to estimate the additional heat flux associated with this parameterization. The anthropogenic heat flux associated with space heating, noted Q_{Fsh}, is estimated, using the following equation, as a weighted average of the heat fluxes between the building interior and the internal layer of the wall and between the building interior and the internal layer of the roof when the internal temperature is set to its minimum value of 19 °C:

$$Q_{\mathrm{Fsh}} = \frac{S_{\mathrm{wall}} \frac{1}{R_i} (T_{i\min} - T_{\mathrm{iw}}) + S_{\mathrm{roof}} \frac{1}{R_i} (T_{i\min} - T_{\mathrm{ir}})}{S_T},$$

where Q_{Fsh} is the anthropogenic heat flux associated with space heating (W m^{-2}), S_{wall} is

the area of the wall, S_{roof} is the area of the roof, $T_{i\,\min}$ is the minimum building internal temperature T_{iw} is the internal wall layer temperature, T_{ir} is the internal roof layer temperature, R_i is the aerodynamic resistance for the inside of the building equal to $0.123\,\text{K}\,\text{m}^2\,\text{W}^{-1}$ (Masson et al. 2002) and S_T is the total area of the canyon. For comparison with the inventory of energy consumption, this flux has been averaged over daily periods.

2.5 TEB implementation

TEB has been run for two periods of the CAPITOUL field program during which Q_F has a strong contribution: a fall period from 15 October to 15 November 2004 and then a winter period from 15 January to 15 February 2005. Forcing observations have been averaged over 30 min. The TEB time step was fixed to 5 min and outputs are averaged over 30 min periods. Since the con-

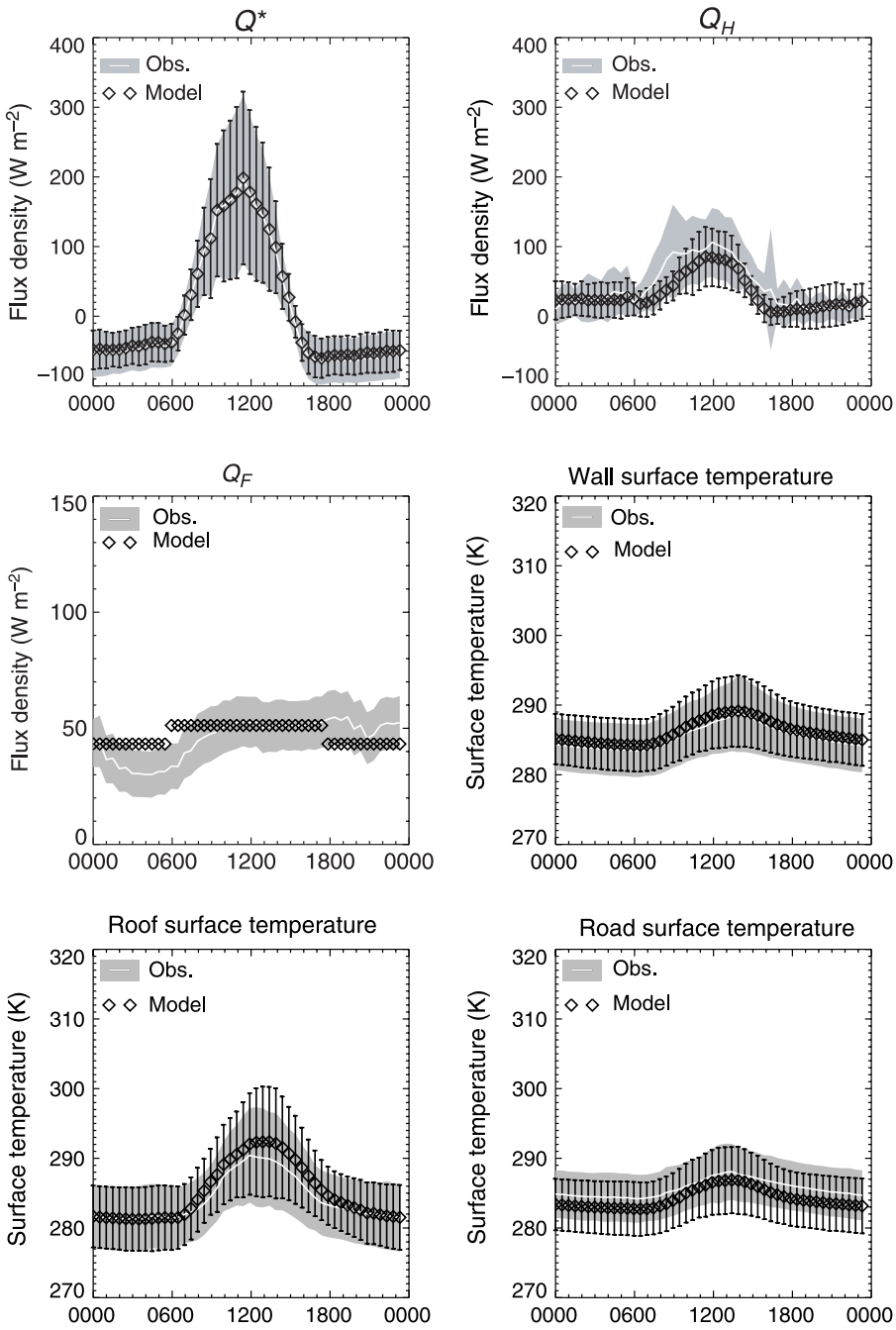

Fig. 1. Ensemble average daily cycle of net radiation (top left), sensible heat flux (top right), anthropogenic heat flux (middle left), wall surface temperature (middle right), roof surface temperature (bottom left) and road surface temperature (bottom right) for the fall period simulation. Standard deviations are represented by grey shaded area (observations) and error bars (model)

ditions are always unstable to neutral (see Q_H on Fig. 1), the footprint area of the measurements at 28 m will not have a spatial extension larger than 500 m according to Lemonsu et al. (2004, 2008). Moreover, the urbanisation around the surface energy balance station is very homogeneous. Consequently, the model has been run over the 500-m radius circle around this station since this can be considered within its footprint for the different variables that we evaluate in this study.

3. Results and discussion

Net radiation and sensible heat flux computed with the simulation have been compared with the observations of the same parameters on the

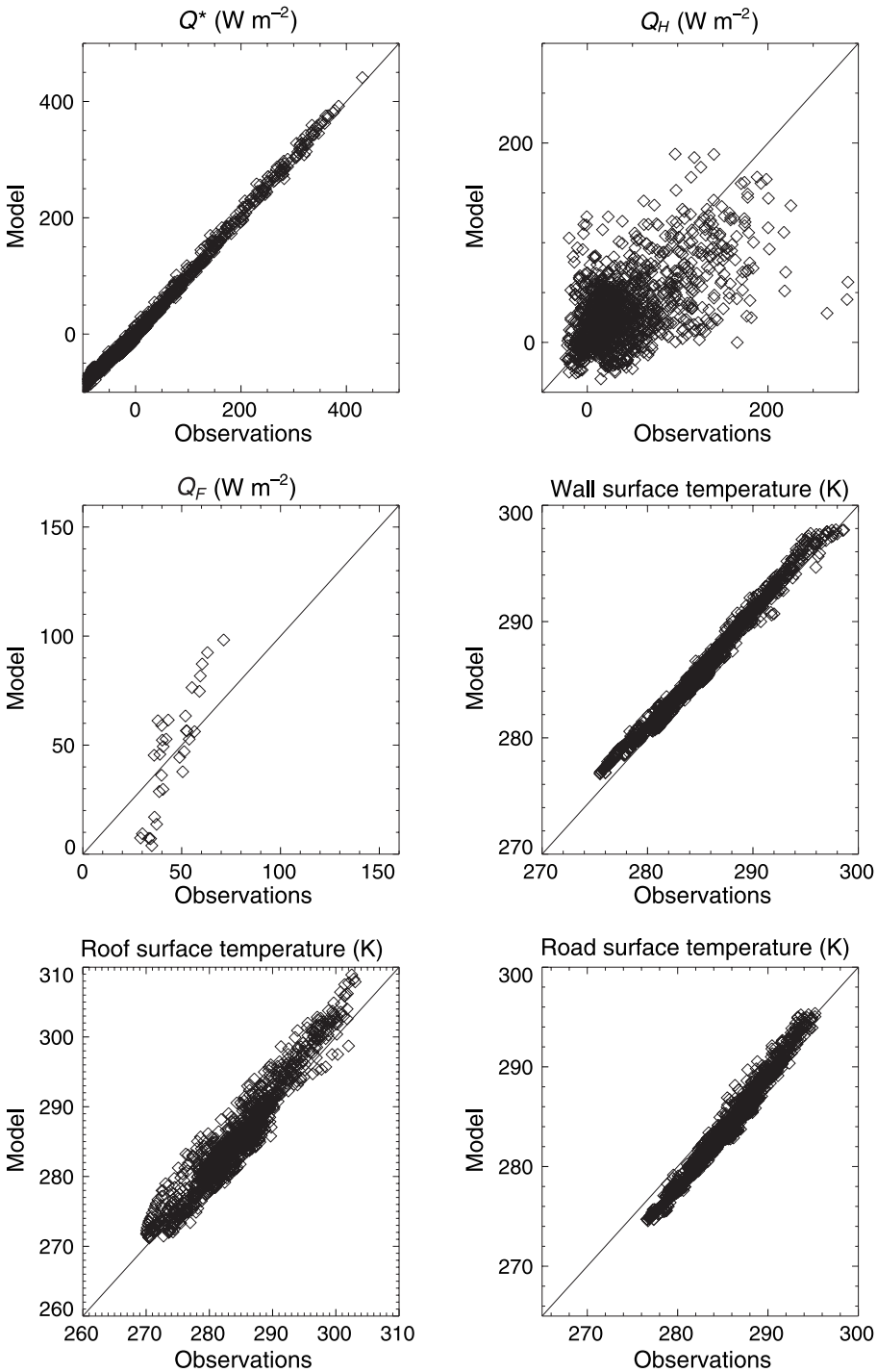

Fig. 2. Scatter plots of model predictions versus observations of net radiation (top left), sensible heat flux (top right), anthropogenic heat flux (middle left), wall surface temperature (middle right), roof surface temperature (bottom left) and road surface temperature (bottom right) for the fall period simulation

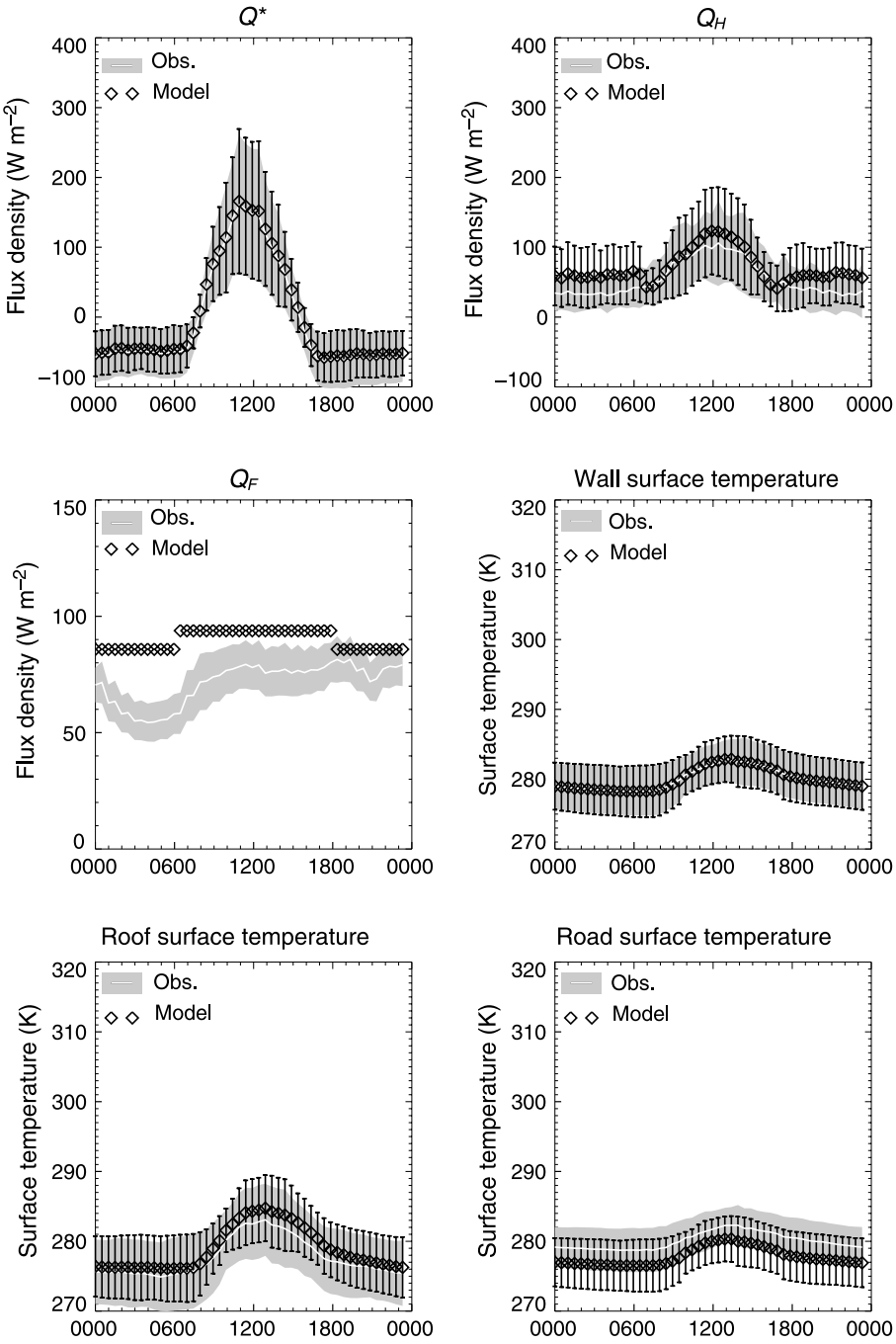

Fig. 3. Ensemble average daily cycle of net radiation (top left), sensible heat flux (top right), anthropogenic heat flux (middle left), wall surface temperature (middle right), roof surface temperature (bottom left) and road surface temperature (bottom right) for the winter period simulation. Standard deviations are represented by grey shaded area (observations) and error bars (model)

micrometeorological tower. The estimate of anthropogenic heat flux computed from the model is compared to the inventory of energy consumption. Mean diurnal cycles of these outputs, as well as the surface temperatures of the wall, the roof and the road, are presented in Figs. 1 and 3 for fall and winter respectively. These diurnal cycles have been computed by taking into account only the samples when the observations were available. Scatter plots of the same measured and modelled variables are presented in Figs. 2 and 4 for fall and winter, respectively. Scores for the same parameters for both seasons computed as bias and Root Mean Square Difference (RMSD) are presented in Table 4.

3.1 Fall period

During fall, the behaviour of the model is very good for Q^* and suggests a good performance

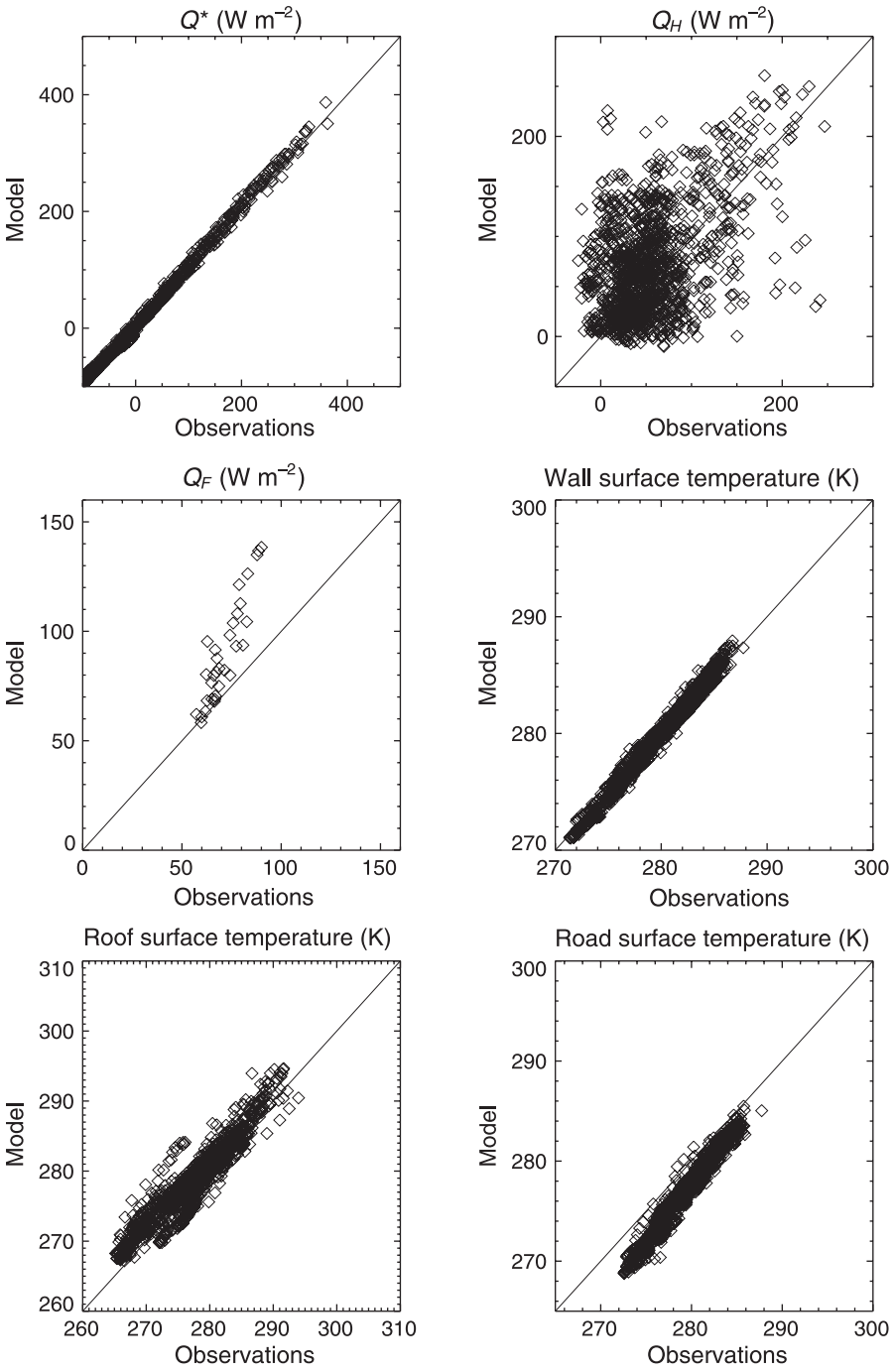

Fig. 4. Scatter plots of model predictions versus observations of net radiation (top left), sensible heat flux (top right), anthropogenic heat flux (middle left), wall surface temperature (middle right), roof surface temperature (bottom left) and road surface temperature (bottom right) for the winter period simulation

Table 4. Bias and RMSD between the model and the observations for the two simulation periods

		Q^* (W m^{-2})	Q_H (W m^{-2})	Q_F (W m^{-2})	$T_{S_{wall}}$ (K)	$T_{S_{roof}}$ (K)	$T_{S_{road}}$ (K)
Fall	Bias	4	−11	2	0.8	1.0	−1.4
(15/10/04-15/11/04)	RMSD	8	44	23	0.9	2.1	1.6
Winter	Bias	5	16	18	0.0	1.2	−2.2
(15/01/05-15/02/05)	RMSD	7	52	28	0.5	2.2	2.4

for the albedo since both shortwave and longwave radiation are input into TEB. The mean daily cycle (Fig. 1, top left graph) is very well reproduced and the variability of the model and the observations are comparable. It results in a very low scatter of the model predictions compared to the observations (Fig. 2, top left graph) as well as a small bias and a RMSD lower than $10\,W\,m^{-2}$ (Table 4). This result is consistent with the good ability of the model to represent the surface temperatures. The wall surface temperature is the best reproduced temperature with bias and RMSD lower than 1 K (Table 4). The daily cycle is also well predicted (Fig. 1, middle right graph) and the representation of the model estimates as a function of the observations shows little scatter (Fig. 2, middle right graph). The roof surface temperature is also well simulated by the model even if it is slightly overestimated during the day (Fig. 1, bottom left graph) or more generally for the highest values (Fig. 2, bottom left graph). The road surface temperature is slightly underestimated by the model by 1.5 K on average (Table 4). This underestimation is larger during the night than during the day (Fig. 1, bottom right graph). The lowest road surface temperatures are under-estimated by the model while the highest temperatures are generally well reproduced in the simulation (Fig. 2, bottom right graph). The ensemble average daily cycle of Q_H over the period (Fig. 1, top right) is very well represented by the model and only a small negative bias of the model computed for this flux (Table 4) is noted. On Fig. 1, the Q_F estimates for the model (middle left graph) are the superposition of the mean value of the heat releases associated with space heating during the period and the heat releases associated with traffic. Concerning the estimates of Q_F calculated from the inventory of energy consumption, the ensemble average daily cycle is presented. On Fig. 2, the scatter plot of the daily average fluxes are represented and it can be seen that the model has a tendency to be too dynamic compared to the observations (middle left graph) under-predicting the lowest values and over-predicting the highest Q_F values. Nevertheless, the important result here is the good reproduction by the model of the mean value of Q_F with a difference between both averages of $1\,W\,m^{-2}$ (Table 5). To conclude, for the evaluation of TEB during the fall, it is important to note its ability to reproduce the specific observed characteristics of the urban energy balance such as the slightly positive sensible heat flux during the night period that is probably associated with a strong contribution of the heat releases associated with space heating.

Table 5. Comparison between estimates of the anthropogenic heat flux in the observations and in the model

	Q_F ($W\,m^{-2}$) observations	Q_F ($W\,m^{-2}$) simulation
Fall (15/10/04-15/11/04)	46	47
Winter (15/01/05-15/02/05)	71	90

3.2 Winter period

During winter, TEB still reproduces a very good Q^*. This is the case for its ensemble average daily cycle (Fig. 3, top left graph) and also for most of the samples during this period as can be seen on the scatter plot between the model and the observations (Fig. 4, top left graph). It results in a RMSD for this flux that is still lower than $10\,W\,m^{-2}$ (Table 4). This result is still associated with a generally good ability of the model to reproduce the surface temperatures, especially the wall surface temperature for which there is a very low RMSD between the model and the observations (Table 4), as well as a good ensemble average daily cycle (Fig. 3, middle right graph). However, it can be seen that TEB has a tendency to underestimate the road temperature by slightly more than 2 K (Table 4). Figure 4 (bottom right graph) shows that this underestimation is more accentuated for the lowest values of the road surface temperature. On the other hand, the magnitude of the daily cycle is, on average, well reproduced (Fig. 3, bottom right graph). At the same time, the model has a slight tendency to predict higher roof surface temperatures than those observed (Fig. 3, bottom left graph). This is the case during the middle of the day and it certainly results in the slight overestimation of Q_H by the model for the same hours (Fig. 3, top right graph). The model also has a tendency to predict slightly larger values of Q_H during the night hours and the releases associated with the

space heating are generally too high (Fig. 3, middle left graph and Table 4). This behavior of the model is particularly true for the highest values of Q_F (Fig. 4, middle left graph). Despite these differences between the model and the observations, TEB is generally able to reproduce the order of magnitude of this term during winter (approximately 80 W m^{-2}) and the processes associated with this term: building surface temperatures higher than air temperature and positive heat flux during night periods.

4. Conclusions

In this study an evaluation of the TEB model has been performed against the CAPITOUL field data set collected over Toulouse. The model has been run in an offline mode forced by the meteorological parameters observed at the top of a tower in the dense old centre of Toulouse. The evaluation has been conducted against the energy fluxes measured at the top of the same tower and the surface temperatures measured with infra-red thermometers for a selected set of walls, roads and roofs with different orientations and aspect ratios. The model has been run for two different periods of the field program: one month in fall and one month in winter. For these two periods, the model reproduces well the most important characteristic of the urban surface energy balance: the strong contribution of sensible heat flux with small positive values during the night associated with high values of the anthropogenic heat flux. This last point is important since this study is the first attempt to evaluate the TEB parameterization of the space heating against an inventory of energy consumption built with a high spatial and temporal resolution over the agglomeration of Toulouse.

It will be interesting to test, when TEB is coupled to a three dimensional atmospheric model, if the ability of the urban scheme to reproduce strong anthropogenic heat releases and positive values of the sensible heat flux during the night can lead to the reproduction of typical nocturnal urban boundary layer structures like the cross-over of vertical profiles of air temperature (Oke 1987) in comparison to a rural profile. Another interesting application of the ability of TEB to correctly reproduce the anthropogenic heat releases is the possibility to use it for the forecast of the energy demand for space heating at the scale of a city.

Appendix A

Correction of the influence of traffic on road surface temperature measurements with infra-red thermometers

Infra-red thermometers (IRT) measuring road surface temperature during CAPITOUL were set up between the middle and the top of the walls to get a large representative field of view (FOV) of the canyon road surface. Consequently, it was possible for vehicles to pass through the FOV of the instrument. High frequency observations made during the initial set-up of CAPITOUL as well as observations from the BUBBLE campaign (Rotach et al. 2005) showed individual sample temperatures decreasing by up to 4 °C due to the presence of a vehicle within the FOV of the IRT. This effect was attributed to the presence of relatively low emissivity materials that characterize some vehicles. These materials include polished metal, glass, and aluminum, the latter of which is used in some truck trailer bodies. When a low emissivity surface obstructs the view of the road, the measured IRT will be influenced by both the emission by the obstruction and its reflection of incident radiation. TEB and other urban canyon models estimate a canyon floor temperature, so for best comparison between observed and modeled temperatures, the effect of traffic must either be (i) added to the model or (ii) removed from the observations. Here we describe a method for removing the traffic influence from CAPITOUL observations.

Because traffic effects on the apparent surface temperature had been noted during the set-up of CAPITOUL, the IRTs were sampled at 1 s intervals and the samples were stored in histograms (covering a 15 min period) with 12 class intervals of 0.5 °C wide each set to cover ±3.0 °C from the mean temperature of the previous 15 min averaging period. This approach provided a compromise between the demands of data storage for storing individual samples and the loss of information associated with storing just a mean value. The histograms were merged to hourly histograms.

The correction procedure uses traffic count data to determine the probability that the FOV is occupied by a vehicle. The probability that the FOV is obstructed is based on: (i) the size of projected FOV, (ii) vehicle size, (iii) vehicle speed, and (iv) sampling rate of the IRT. A threshold of 20% FOV obstruction is used to determine affected samples. The number of affected samples (N_{cor}) is determined as:

$$N_{\mathrm{cor}} = \mathrm{TC}\, Pob_{0.2}$$

where TC is the traffic count and $Pob_{0.2}$ is the probability of 20% FOV obstruction. Traffic counts were provided from an automated traffic counter located near the Alsace road site; traffic counts for the other sites were linearly related to Alsace road traffic, based on an evaluation of other nearby traffic count data provided by the Transportation Office of Toulouse.

The IRT FOVs were calculated and then approximated by rectangles with dimensions that match the ellipse axes

Table A1. Characteristics of the field of view of the infra-red thermometer for each road

Canyon	Ellipse area (m^2)	Rectangle length (m)	Rectangle width (m)
Alsace	23.25	4.99	4.66
Pomme	21.09	4.66	4.53
Rémusat	4.40	2.52	1.75

Table A2. For each road, figures necessary to determine the number of samples to discard from the data set

Road	Probability of a moving vehicle occupies 20% of the FOV	Typical number of vehicles per hour	Typical number of lowest samples to eliminate per hour
Alsace	0.41	700	287
Pomme	0.65	280	182
Rémusat	0.51	310	158

(Table A1). The average vehicle size was estimated as 4.5 m in length and 2.0 m in width. Vehicle speed was set at $40\,km\,h^{-1}$ ($11.1\,m\,s^{-1}$).

For two of the roads (Pomme and Rémusat), a lane devoted to parking was in the FOV of the IRTs and a vehicle parked on this lane occupies a fraction of the 20% of the FOV. It has been assumed that this lane was occupied 75% of the time and in this case, the probability that a moving vehicle occupies the necessary additional area to reach 20% of the FOV has been estimated with the same method as presented before. For each road, the total probabilities that a moving vehicle occupies more than 20% of the FOV (P_{20}) are presented in Table A2.

Since the presence of a vehicle in the FOV typically leads to a lower reading, the N_{cor} lowest samples have been discarded and a new mean temperature has been calculated without these samples. The typical values of traffic intensity and number of samples to discard are presented in Table A2.

References

ASHRAE (1989) ASHRAE Handbook: 1989 Fundamentals. ASHRAE, 797 pp

Batchvarova E, Gryning S (2006) Progress in urban dispersion studies. Theor Appl Climatol 84: 57–67

Best MJ (2006) Progress towards better weather forecasts for city dwellers: from short range to climate change. Theor Appl Climatol 84: 47–55

Grimmond CSB, Oke TR (1999a) Heat storage in urban areas: observations and evaluation of a simple model. J Appl Meteorol 38: 922–40

Grimmond CSB, Oke TR (1999b) Aerodynamic properties of urban areas derived from analysis of surface. J Appl Meteorol 38: 1262–92

Hallegatte S, Hourcade J, Ambrosi P (2007) Using climate analogues for assessing climate change economic impacts in urban areas. Clim Change 82: 47–60

Hamdi R, Schayes G (2005) Validation of the Martilli's urban boundary layer scheme with measurements of two mid-latitude European cities. Atmos Chem Phys Dis 5: 4257–89

Kobayashi T, Takamura T (1994) Upward longwave radiation from a non-black urban canopy. Bound Layer Meteorol 69: 201–13

Krayenhoff ES, Voogt JA (2007) A micro-scale 3-D urban energy balance model for studying surface temperatures. Bound Layer Meteorol 123: 433–61. DOI: 10.1007/s10546-006-9153-6

Ichinose T, Shimodozno K, Hanaki K (1999) Impact of anthropogenic heat on urban climate in Tokyo. Atmos Environ 33: 3897–909

Lemonsu A, Grimmond CSB, Masson V (2004) Modelling the surface energy balance of an old Mediterranean city core. J Appl Meteorol 43: 312–27

Lemonsu A, Bélair S, Mailhot J, Benjamin M, Chagnon F, Morneau G, Harvey B, Voogt JA, Jean M (2008) Overview and first results of the montreal urban snow experiment 2005. J Appl Meteorol Climatol 47: 59–75

Masson V (2000) A physically-based scheme for the urban energy budget in atmospheric models. Bound Layer Meteorol 94: 357–97

Masson V (2006) Urban surface modelling and the meso-scale impact of cities. Theor Appl Climatol 84: 35–45

Masson V, Grimmond CSB, Oke TR (2002) Evaluation of the Town Energy Balance (TEB) scheme with direct measurements from dry districts in two cities. J Appl Meteorol 41: 1011–26

Masson V, Gomes L, Pigeon G, Liousse C, Pont V, Lagouarde J-P, Voogt J, Salmond J, Oke TR, Hidalgo J, Legain D, Garrouste O, Lac C, Connan O, Briottet X, Lachérade S, Tulet P (2008) The Canopy and Aerosol Particles Interactions in TOulouse Urban Layer (CAPITOUL) experiment. Meteorol Appl Phys 102: 135–57

McMillen RT (1988) An eddy correlation technique with extended applicability to non-simple terrain. Bound Layer Meteorol 43: 231–45

Moscicki MA (2007) A comparison of modelled and observed urban surface temperatures in Toulouse, France. Unpublished M.Sc. Thesis, The University of Western Ontario, London, ON, Canada, 171 pp

Noilhan J (1981) Contribution à l'étude du microclimat au voisinage d'un bâtiment, Ph.D. Thesis, Université Paul Sabatier, Toulouse, 160 pp

Noilhan J, Planton S (1989) A simple parameterization of land surface processes for meteorological models. Mon Wea Rev 117: 536–49

Offerle B, Grimmond CSB, Fortuniak K (2005) Heat storage and anthropogenic heat flux in relation to the energy balance of a central European city centre. Int J Climatol 25: 1405–19

Oke TR (1987) Boundary layer climates, 2nd edn. Methuen, New York and London

Oke TR (2006) Towards better scientific communication in urban climate. Theor Appl Climatol 84: 179–90

Pigeon G, Legain D, Durand P, Masson V (2007) Anthropogenic heat release in an old European agglomeration (Toulouse, France). Int J Climatol 27: 1969–81

Roberts SM, Oke TR, Grimmond CSB, Voogt JA (2006) Comparison of four methods to estimate urban heat storage. J Appl Meteorol Climatol 45: 1766–81

Rotach MW, Vogt R, Bernhofer C, Batchvarova E, Christen A, Clappier A, Feddersen B, Gryning S-E, Martucci G, Mayer H, Mitev V, Oke TR, Parlow E, Richner H, Roth M, Roulet Y-A, Ruffieux D, Salmond JA, Schatzmann M, Voogt JA (2005) BUBBLE – an Urban Boundary Layer Meteorology Project. Theor Appl Climatol 81: 231–61

Sailor DJ, Lu L (2006) A top-down methodology for developing diurnal and seasonal anthropogenic heating profiles for urban areas. Atmos Environ 38: 2737–48

Voogt JA, Oke TR (1998) Radiometric temperatures of urban canyon walls obtained from vehicle traverses. Theor Appl Climatol 60: 199–217